Indian Journal of Chemical Technology
Vol. 25, March 2018, pp. 189-195

Electrocatalytic activity of $Ni_xFe_{3-x}O_4$ ($0 \leq x \leq 1.5$) film electrode for oxygen evolution in KOH solutions

Ritu Yadav & Narendra Kumar Singh*

Department of Chemistry, Faculty of Science, University of Lucknow, Lucknow 226 007, India

E-mail: nksbhu@yahoo.com, singh_narendra@lkouniv.ac.in

Received 3 June 2016; accepted 15 February 2018

Spinel-type pure and Ni-substituted ferrites have been synthesised by novel ammonium hydroxide precipitation method at *p*H 11.5 and their electrocatalytic properties have been studied with regards to oxygen evolution reaction (OER) in alkaline solutions. Physicochemical and electrochemical techniques used to characterize the materials are X-ray diffraction (XRD), scanning electron microscope (SEM), infrared (IR), cyclic voltammetry (CV) and anodic polarization (Tafel plot). Results of IR and XRD studies show the formation of spinel phase of the material along with some small impurity. All the electrochemical studies are carried out in a three electrode single compartment glass cell. For the purpose, materials have been transformed in the oxide film electrode by oxide slurry painting technique. The cyclic voltammetric curve of each oxide electrode exhibit redox peaks (anodic: 519 ± 33mV and cathodic: 362 ± 2 mV) prior to the oxygen evolution reaction (OER). The electrocatalytic activity of the material has been determined by recording the anodic polarization curve in 1 M KOH at 25°C. Data show that the Ni-substitution in the base oxide enhance the electrocatalytic activity of the material and value is found to be greatest with 0.5 mol Ni. This material produced overpotential 583 mV at 100 mA cm^{-2} current density. Tafel slope values are ranged between 64-81 mV $decade^{-1}$ with fractional order of reaction. The activation energy and other thermodynamic parameters are also estimated by recording the anodic polarization curve in 1M KOH at different temperatures.

Keywords: Coprecipitaiton, XRD, SEM, Overpotential, Electrocatalysis, Oxygen evolution

The transition metal mixed oxides of Ni and Fe with spinel-type structure are considered to best promising materials and have tremendous biological and technological applications such as magnetically guided drug delivery[1], catalysis[2,3], ferrofluids[4,5], magnetic data storage materials[6], sensors[7], synthesis of ammonia[8], production of chlorate from chlorine[9], selective oxidation of butene[10], decomposition of ammonia[11] etc. over the past half century. These materials have also been found to be good electrocatalysts for electrolytic evolution/reduction of oxygen in alkaline solutions. It is noteworthy that the interfacial properties play a key role in heterogeneous catalysis and are strongly depend upon different variables such as the nature of precursors, methodology and temperature. Various methods, which give the possibilities to provide materials having different particle size, have been reported in literature. Among them, thermal decomposition[12-18] and freeze-drying[19-21] require relatively high temperature and produced oxides of larger particle size. The low temperature methods like hydrothermal[22], co-precipitation[23-28], sol-gel[29-34] etc. produced materials of high specific surface area with low particle size. Recently, Singh *et al*[24,35-40] reported a series of metal substituted binary as well as ternary spinel ferrites obtained by sodium hydroxide precipitation method at *p*H 11.0 and studied their electrocatalytic properties towards oxygen evolution reaction (OER) in alkaline solution. The results showed a great enhancement in the electrocatalytic activity of these materials as compared to that obtained by higher temperature methods.

The above studies prompted us to develop pure and Ni-substituted spinel ferrites by adopting ammonium hydroxide precipitation method and investigated their electrochemical properties for oxygen evolution reaction in alkaline solution. In the present paper we used metal chlorides and aqueous ammonia solution as precursors and precipitating agent, respectively. Results, so obtained are described below.

Experimental Section

Spinel-type binary oxides of Fe and Ni having general formula $Ni_xFe_{3-x}O_4$ ($0 \leq x \leq 1.5$) were prepared by coprecipitaionmethod.In each preparation, all the chemicals used were of analytical grade and purified. The stoichiometric quantity of chlorides of Fe [$FeCl_3.6H_2O$ (purified, Merck 96%)] and Ni [$NiCl_2.6H_2O$ (purified, Merck 97%)] were

dissolved in 100 mL double distilled water. The *p*H of the solution was adjusted to 11.5 by adding NH_4OH (25%, Fischer) drop wise. The precipitate, so obtained, was filtered and washed with double distilled water till free from chloride ions and finally dried at 100°C for 24 h. The dried precipitate was crushed in agate pastel mortar to transfer it into fine powder and then sintered at 400°C 5 h in PID controlled electrical furnace (ASco, India) to get the desired oxides.

The spinel phase of the oxide powder was confirmed by IR (FT-IR Thermoscientific; Nicole-6700) and X-Ray diffraction (Bruker D-8 advanced series-2 diffractometer) using Cu-Kα_1 as the radiation source (λ = 1.54056 Å). The Scanning electron microscope (SEM; Jeol JSM 6490) was used to know the morphology of the synthesized oxide in powder. All the electrochemical studies have been performed in the three electrode single compartment glass cell. For the purpose, the oxide powder was first transformed in the form of film electrode on a pre-treated Ni-support (Sigma-Aldrich, 99.9%) by an oxide slurry painting method[41]. The preparation of slurry and electrical contact with the oxide film to make the electrode have been performed in the similar way as described in literature[41].

All the electrochemical characterization namely, Cyclic voltammogram (CV) and Tafel polarization curve were carried out by using an electrochemical Impedance system (Gamry Reference 600 ZRA) provided with potentiostat/galvanostat and a corrosion and physical electrochemistry software installed personal computer (PC) system (hp). The reference and auxiliary (counter) electrodes were Hg/HgO in 1 M KOH (E° = 0.098 V vs NHE) and pure Pt-foil of relatively large geometrical surface area (~ 2 cm^2), respectively. The working electrode was the oxide film electrode. The potential of the working (test) electrode was measured with respect to Hg/HgO/1 M KOH reference electrode. In order to minimize the solution resistance (iR drop) between the working and the reference electrode, the reference electrode was connected to the cell solution through the luggin capillary (the KCl/Agar-Agar salt bridge). The value of overpotential, as mentioned in the text, was calculated by using relation, $\eta = E - E_{O_{2/OH^-}}$, where, E is the applied potential across the catalyst/1M KOH interface and $E_{O_{2/OH^-}}$ (= 0.303 V vs. Hg/HgO) represents the theoretical equilibrium Nernst potential in 1 M KOH at 25°C.

Results and Discussion

SE-micrographs of pure and Ni-substituted oxide powder, sintered at 400°C for 5 h, were carried out at different magnifications and represented in Fig. 1 (A-D) at magnification × 500. Figure shows that appearance of oxide powder is almost similar except $Ni_{0.5}Fe_{2.5}O_4$ oxide, which indicates amorphous and cloudy structure with smaller grain size. Morphologies of other material consist of relatively large particle size.

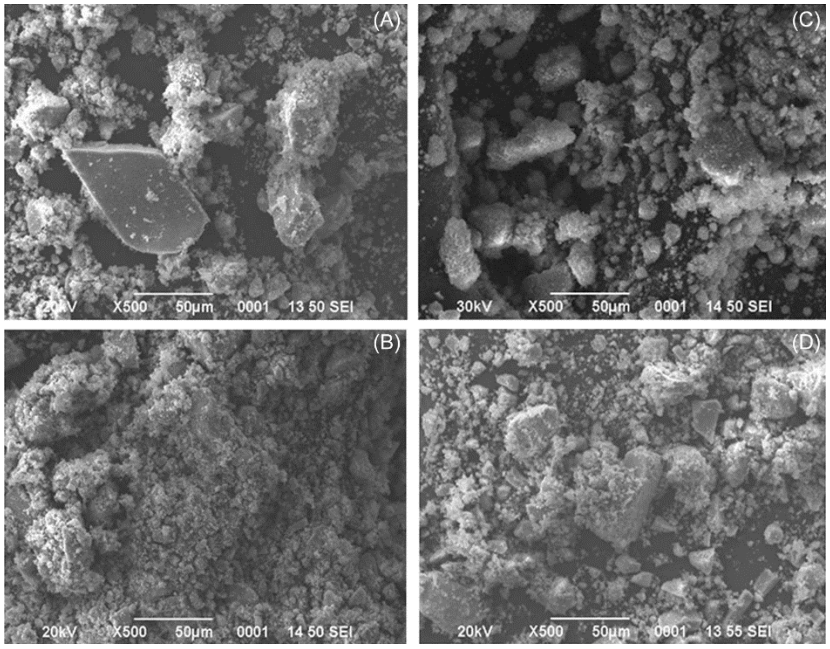

Fig. 1 — SE-Micrographs of oxide powder sintered at 400°C, 5 hrA: Fe_3O_4, B: $Ni_{0.5}Fe_{2.5}O_4$, C: $NiFe_2O_4$, D: $Ni_{1.5}Fe_{1.5}O_4$.

IR spectra of $Ni_xFe_{3-x}O_4$ (x = 0.5, 1.0 and 1.5) oxide powder obtained at 400°C, has been recorded over the frequency range 4000-400 cm^{-1} in KBr medium. Two absorption bands at ~ 580 and ~ 460 cm^{-1} as observed in the figure indicates the characteristic bands of pure spinel ferrites[42-44]. The intense broad peak at ~ 3400 cm^{-1} and a small peak at ~ 1623 cm^{-1} indicate the O-H stretching vibrations interacting through H-bond. These absorption bands are ascribed due to the hygroscopic nature of the material prepared at relatively low temperature.

The XRD powder patterns of the oxide, sintered at 400°C 5 hrs, with x = 0 and x = 1.5 were recorded between 2θ = 20° and 80° and the spectra, thus obtained, are shown in Fig. 2. The observed 2θ and the corresponding 'd' values were analysed by using JCPDS ASTM file 01-1053 and 44-1485 for Fe_3O_4 and $NiFe_2O_4$, respectively and found to be closely matched with the literature and follow almost cubic crystal geometry. However, spectra show some additional diffraction lines corresponding to 'd' values 1.84, 2.69 and 3.68 Å of Fe_2O_3 (JCPDS ASTM Card 01-1053) as impurities. Values of crystallite size were found to be 32 and 24 nm for Fe_3O_4 and $Ni_{1.5}Fe_{1.5}O_4$, respectively, estimated by using Scherer's formula[45].

Cyclic voltammetry

Cyclic voltammograms of oxide film electrodes on Ni were carried out in the potential region between 0.0-0.7 V at a scan rate of 20 mV sec^{-1} in 1 M KOH at 25°C. Voltammetric curves, so obtained, for each oxide electrode, are shown in Fig. 3. Each voltammogram shown in Fig. 3exhibited a pair of redox peaks, one anodic (519 ± 33 mV) and a corresponding cathodic (362 ± 2 mV) peak prior to the oxygen evolution reaction. The peak separation potential and formal redox potential calculated from the CV curves were found to be 158 ± 32 and 440 ± 17 mV, respectively. Other cyclic voltammetric parameters like, anodic peak current (j_{Pa}), cathodic peak current (j_{Pc}) and charge (q) are also estimated from the CV curve. Data, so obtained, are shown in Table 1. The ratio of anodic peak and cathodic peak current was found to be ~2. This indicates the irreversibility of the redox process. The voltammetric charge (q) is increased with Ni-substitution in the base oxide and value was found to be maximum with 0.5 mol Ni.

Further, it has been observed that the cyclic voltammogram of 0.5 mol Ni-substituted ferrite film on Pt-support did not indicate any redox peaks before the commencement of OER. This indicates that the redox peaks produced at the oxide film electrode on Ni were originated from the Ni-support and not from the oxidation-reduction of the oxide film. The effect of scan rate on the voltammetric parameters has also been tested with each oxide electrode. For the purpose, the cyclic voltammogram was recorded at various scan rates ranging from 20-120 mV sec^{-1} (Fig. 4). The nature of curves obtained at different scan rates was found to be similar. However, the anodic and cathodic peak shifted either side when scan rate increases from 20 to 120 mV sec^{-1}. Also, it is observed that the voltammetric charge goes on decreasing with increasing in scan rates. The plot of voltammetric charge as a function of $(\text{scan rate})^{-1/2}$, as shown in the Fig. 5, was observed to be linear with each oxide electrocatalyst. This indicates that the surface redox process is diffusion control.

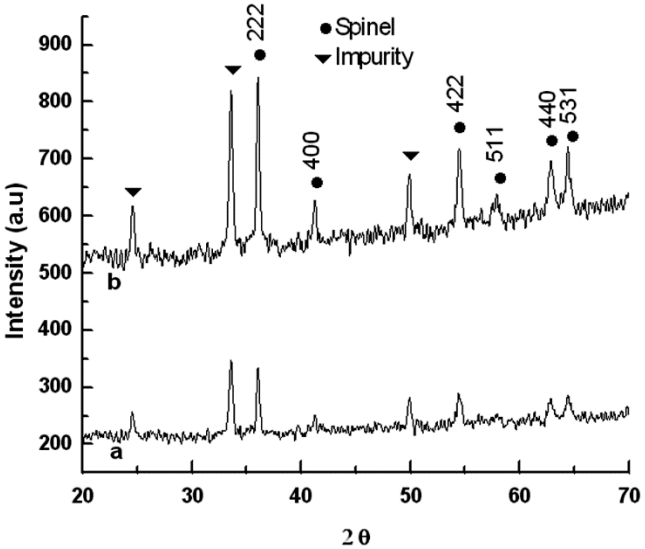

Fig. 2 — XRD powder patterns of $Ni_xFe_{3-x}O_4$, sintered at 400°C for 5 h; (a) x = 0 mol (b) x = 1.5 mol

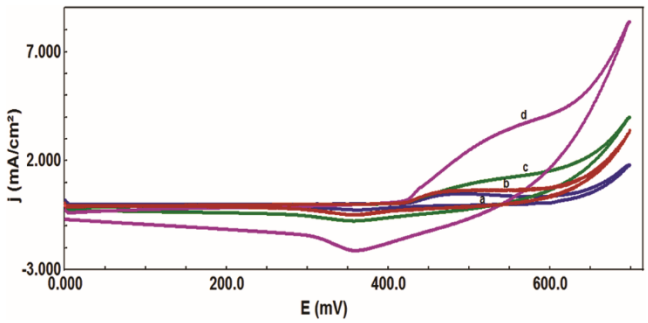

Fig. 3 — Cyclic voltammograms of pure and Ni-substituted ferrite film electrodes on Ni at 20 mV sec^{-1} scan rates in 1M KOH (25°C) a: Fe_3O_4, b: $NiFe_2O_4$, c: $Ni_{1.5}Fe_{1.5}O_4$, d: $Ni_{0.5}Fe_{2.5}O_4$.

Table 1 —Values of the cyclic voltammetric parameters of $Ni/Ni_xFe_{3-x}O_4$ ($0 \le X \le 1.5$) in 1 M KOH at 25°C (scan rate = 20 mV sec^{-1})

Electrode	E_{Pa} /mV	E_{Pc} /mV	ΔE_P /mV	$E°= (E_{Pa} + E_{Pc})/2$ /mV	$\|j_{Pa}\|$ /mA cm^{-2}	$\|j_{Pc}\|$ /mA cm^{-2}	$\|j_{Pa}\|/ \|j_{Pc}\|$	q / mCcm^{-2}
Fe_3O_4	486	360	126	423	0.5	0.3	1.9	5.7
$Ni_{0.5}Fe_{2.5}O_4$	552	362	190	457	3.7	2.1	1.7	49.6
$NiFe_2O_4$	540	363	177	452	1.1	0.8	1.5	17.7
$Ni_{1.5}Fe_{1.5}O_4$	550	362	188	456	3.5	2.1	1.7	48.5

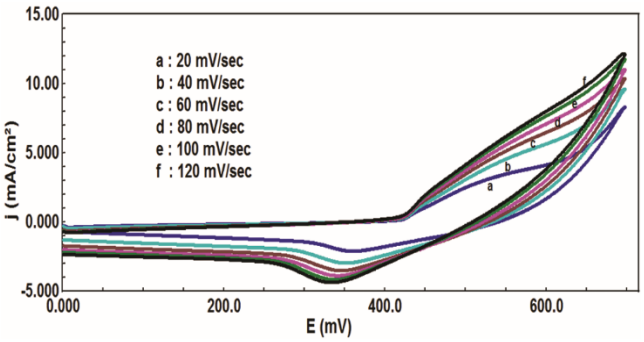

Fig. 4 — Cyclic voltammograms of the $Ni_{0.5}Fe_{2.5}O_4$ film electrode on Ni at different scan rates in 1M KOH (25°C)

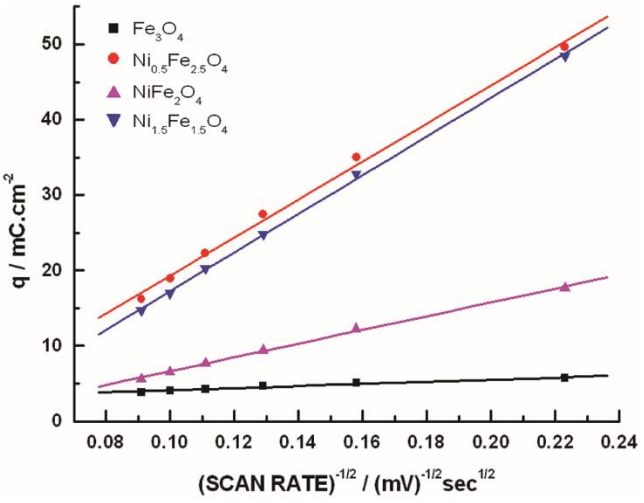

Fig. 5—Plot of voltammetric charge (q) vs. (scan rate)$^{-1/2}$ of the oxide film electrode on Ni (25°C)

Electrocatalytic activity

The electrocatalytic activity of oxide electrode for the OER was examined by recording the anodic polarization curves at scan rate of 0.2 mV sec^{-1} in 1 M KOH at 25°C. Anodic polarization curves (E vs. log j), so obtained, for each oxide electrode are shown in Fig. 6. Values of the Tafel slope (b), the current density at three different overpotential (347, 447 and 547 mV) as well as overpotential at two different current density (10 and 100 mA cm^{-2}) were estimated from the curve and are given in Table 2. Figure 6 and Table 2 demonstrate that the nature of Tafel lines seems to be similar regardless of Ni-substitution in the Fe_3O_4

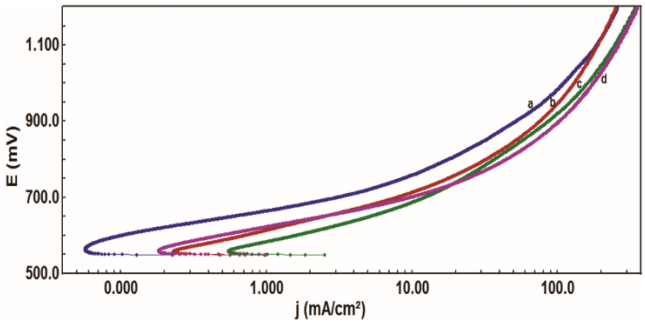

Fig. 6 — Tafel plots for the pure and Ni-substituted ferrite films on Ni in 1M KOH (25°C); scan rate: 0.2mVsec^{-1}, a: Fe_3O_4, b: $NiFe_2O_4$, c: $Ni_{1.5}Fe_{1.5}O_4$, d: $Ni_{0.5}Fe_{2.5}O_4$.

lattice. Further, it has been observed that among all the catalysts, the electrocatalytic activity of $Ni_{0.5}Fe_{2.5}O_4$ was found to be greatest. The Tafel slope values were ranged between 64-81 mV $decade^{-1}$. Based on the apparent current density data at certain overpotential (η_{O_2}= 547 mV), the electrocatalytic activity of oxides follows the order:

$Ni_{0.5}Fe_{2.5}O_4$ (j_a = 75.8 mAcm^{-2}) > $Ni_{1.5}Fe_{1.5}O_4$ (j_a = 58.3 mAcm^{-2}) > $NiFe_2O_4$ (j_a = 53.6 mAcm^{-2}) >Fe_3O_4 (j_a = 39.8 mAcm^{-2})

Based on the oxygen overpotential data at the current density of 100 mA cm^{-2} in 1 M KOH at 25°C, the electrocatalytic activity of oxide electrodes follow the order:

$Ni_{0.5}Fe_{2.5}O_4$ (η_{O_2}= 583 mV) > $Ni_{1.5}Fe_{1.5}O_4$ (η_{O_2} = 616 mV) > $NiFe_2O_4$ (η_{O_2} = 628 mV) > Fe_3O_4 (η_{O_2} = 671 mV)

The order of reaction with respect to [OH^-] was determined with each oxide electrode. For the purpose, the E vs j plot was recorded at varying KOH concentrations at 25°C by keeping the ionic strength (μ = 1.5) of the medium constant. An inert electrolyte KNO_3 (Merck, purified) was used to maintain the ionic strength of the medium constant. A representative plot for $Ni_{0.5}Fe_{2.5}O_4$ at different KOH concentration is shown in Fig. 7. Data collected from the polarization curves were used to construct log j vs. log [OH^-] (Fig. 8) at a constant applied potential (E = 650 mV). The order of reaction was estimated from theslope of

Table 2—Electrode kinetic parameters for oxygen evolution reaction on $Ni/Ni_xFe_{3-x}O_4$($0 \le x \le 1.5$) electrodes in 1 M KOH at 25°C (scan rate = 0.2 mV sec^{-1})

Electrode	Tafel slope / mVd^{-1}	Order (p)	η_{O_2}/ mV at j (mA cm^{-2})		j (mA cm^{-2}) at η_{O_2} / mV		
			10	100	347	447	547
Fe_3O_4	64	1.2	438	671	0.8	11.9	39.8
$Ni_{0.5}Fe_{2.5}O_4$	72	1.3	346	583	2.2	22.3	75.8
$NiFe_2O_4$	81	1.4	406	628	2.8	18.2	53.6
$Ni_{1.5}Fe_{1.5}O_4$	80	1.2	379	616	5.4	23.3	58.3

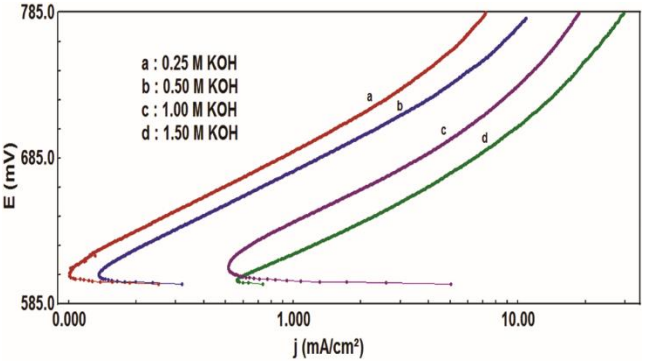

Fig. 7 — Tafel plots for oxygen evolution on the $Ni_{0.5}Fe_{2.5}O_4$ film electrode on Ni at varying KOH concentrations (μ = 1.5) at 25°C.

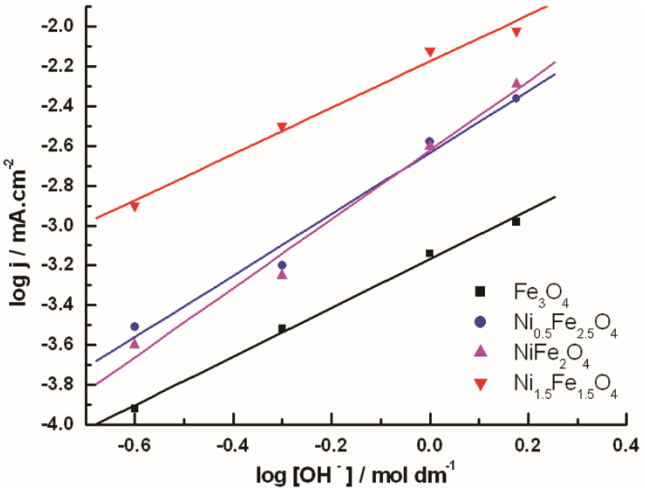

Fig. 8 — Plot of log j vs. log [OH^-] at a constant applied potential (E = 650 mV) for $Ni_xFe_{3-x}O_4$ ($0 \le x \le 1.5$) film electrode on Ni at 25°C

the straight line and values are given in Table 2. The oxide electrode showed almost fractional order of reaction with each oxide electrode. Thus, from the experimentally estimated values of the Tafel slope and order, it is evident that the oxygen evolution reaction follows almost similar mechanistic steps.

It is evident that the electrocatalytic activity of oxide electrodes, especially $Ni_{0.5}Fe_{2.5}O_4$, reported in the present study is observed to be higher than those of other spinel ferrites reported in literature. For example, Iwakura*et al.*[18,46] found η_{O_2} = 440 and 580 mV at j = 10 mA cm^{-2}, on $CoFe_2O_4$ and $MnFe_2O_4$ in 1 M KOH at 25°C, respectively. Orehotsky*et al.*[47] found η_{O_2} = 340 mV on $NiFe_2O_4$ in 30 wt% KOH and Singh *et al.*[37] found η_{O_2} = 368 mV on $CuFe_2O_4$ in 1 M KOH prepared by hydroxide precipitation method at a controlled *p*H (= 11). Very recently, Al. Mayouf*et al.*[48] observed j = 0.62 mA cm^{-2} at E = 650 mV in 1 M KOH at 25°C for Ni ferrite electrode prepared by hydrothermal method.

The effect of temperature on the rate of the electrolytic evolution of oxygen has been investigated by recording the anodic polarization curve in 1 M KOH at different temperature with the oxide electrode *viza* Fe_3O_4, $Ni_{0.5}Fe_{2.5}O_4$ and $Ni_{1.5}Fe_{1.5}O_4$. Arepresentative curve for $Ni_{0.5}Fe_{2.5}O_4$ is shown inFig. 9. The Arrhenius plot log j vs. 1/T as shown in Fig. 10was constructed at different applied potentials. From Fig. 10, it is observed that the value of activation energy decreases with increasing the applied potential. The reduction in activation energy at higher potential is found to be well accord with the relation,$\Delta H^{\circ\neq}_{el}$= $\Delta H^{\circ\neq}$ - $\alpha F\eta$, where, $\Delta H^{\circ\neq}$is the standard enthalpy of activation (=$\Delta H^{\circ\neq}_{el}$at η = 0 or E = E_{rev}) and $\alpha F\eta$ is the electrical contribution. The transfer coefficient (α) was estimated by using the equation α = 2.303RT/bF, where, F is the Faraday constant and b is the Tafel slope of the polarization curve at a certain temperature. The entropy of activation ($\Delta S^{\circ\neq}$) for OER was estimated using the relation given in literature[49].

$$\Delta S^{\circ\neq} = 2.3R\left[\log j + \frac{\Delta H^{\circ\neq}_{el}}{2.3RT} - log(nF\omega C_{OH^-})\right] \quad ...(1)$$

where ω (= k_BT/h; k_B is the Boltzmann constant, h is Plank's constant, T is absolute temperature) is the frequency term, for alkaline water electrolysis number of electron transfer (n) is equal to 2, C_{OH^-} is electrolyte concentration, and F is Faraday's constant. The estimated values of$\Delta H^{\circ\neq}_{el}$, $\Delta H^{\circ\neq}$, $\Delta S^{\circ\neq}$ and α are given in Table 3.Highly negative value of $\Delta S^{\circ\neq}$ indicates the

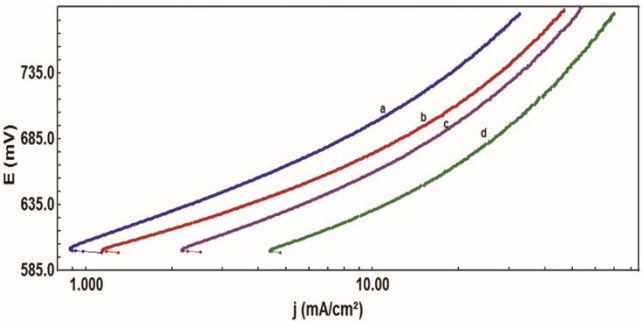

Fig.9 — Tafel plots for oxygen evolution on the $Ni_{0.5}Fe_{2.5}O_4$ film on Ni at different temperatures in 1 M KOH,a: 20°C, b: 30°C, c: 40°C, d: 50°C

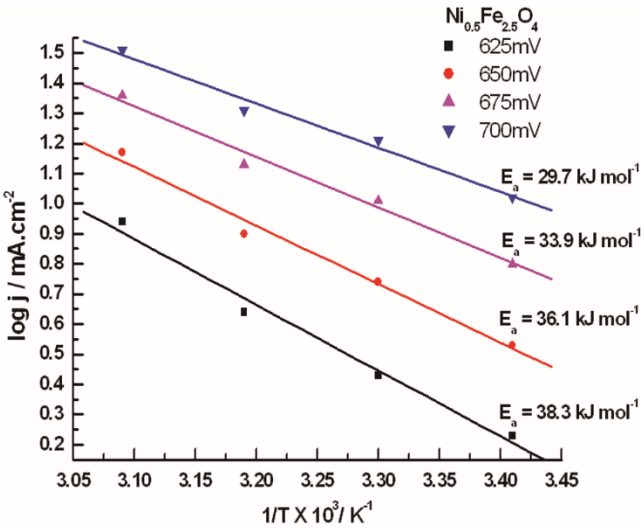

Fig. 10 — Arrhenius plot at different constant applied potentials on $Ni_{0.5}Fe_{2.5}O_4$ in 1 M KOH

Table 3 — Thermodynamic parameters for O_2 evolution on $Ni/Ni_xFe_{3-x}O_4$ ($0 \le x \le 1.5$) in 1 M KOH

Electrode	$\Delta H^{\circ\neq}_{el}$ (KJ mol^{-1}) at E = 675 mV	$-\Delta S^{\circ\neq}$ (J deg^{-1} mol^{-1})	α	$\Delta H^{\circ\neq}$ (KJ mol^{-1})
Fe_3O_4	57.6	162.9	1.0	76.8
$Ni_{0.5}Fe_{2.5}O_4$	38.2	215.7	0.8	63.8
$Ni_{1.5}Fe_{1.5}O_4$	38.4	207.2	0.7	59.9

presence of adsorption phenomenon in the electrochemical formation of oxygen.

Data shown in the Table 3 indicates that the value of activation energy decreases with Ni-substitution. Almost same value to activation energy was observed with 0.5 and 1.5 mol Ni-substitutions. It clearly indicates that the substitution of Ni greatly modifies the energy barrier of reaction towards the enhanced electrocatalytic activity.

Conclusion

The XRD and IR studies of the material indicated the formation of pure spinel ferrite. Results of the electrocatalytic activity have shown that the partial substitution of Ni for Fe in the base oxide greatly enhanced apparent electrocatalytic activity of oxide towards OER. Based on the apparent electrocatalytic scale, $Ni_{0.5}Fe_{2.5}O_4$ has been found to be the best electrocatalysts among the nickel ferrites prepared for the investigation. The catalytic activity of most active electrode was found to be double to the base oxide.

Acknowledgements

Authors are thankful to Dr Jhasaketan,Department of Chemistry, IIT Kanpur, Kanpur for carrying XRD analysis. The Department of Science and Technology (DST), New Delhi for financial support as Fast Track Scheme for Young Scientist (No.: SR/FT/CS–044/2009) are gratefully acknowledged.

References

1 Pulfer S K & Gallo J N, *Scientific and Clinical Applications of magnetic carriers*, edited by U Häfeli, W Schütt, J Teller & M Zborowski, (Plenum Press, New York) 1997, p. 445.
2 Sugimoto M, *J Am Ceram Soc*, 82 (1999) 269.
3 Ramankutty C G &Sugunan S, *ApplCatalA Gen*, 39 (2001) 218.
4 Zarur A J & Ying J V, *Nature*, 403 (2000) 65.
5 Sousa M H, Hasmonay E, Depeyrot J, Tourinho F A, Bacri J C, Dubosis E, Perzyski R, Raikherb Yu L &Magn J, *Mater*, 242 (2002) 572.
6 Raj K & Moskowitz R, *J Magn&Magn Mater*, 233 (1990) 85.
7 Sepelak V, Baabe D, Mienert D, Schultze D, Krumeich F, Litterst F J & Becker K D, *Magn Mater*, 257 (2003) 377.
8 Rajaram R R& Sermon, *J ChemSoc Faraday Trans*, 81 (1985) 2277.
9 Trasatti S & Lodi G, *Electrodes of Conductive Metallic Oxides*, Part B, edited by S Trasatti (Elsevier, Amsterdam) (1981) 569.
10 Harold H K & Mayfair C K, *AdvCatal*, 33 (1985) 159.
11 Kota H M, Katan J, Chim M, Schoenweis, *Nature*, 203 (1964) 1281.
12 Tarasevich M R &Efremov B N, *Electrodes of conductive metallic oxides*, Part A, edited by S Trasatti, (Elsevier, Amsterdam), 1980.
13 Boggio R, Camgati A &Trassati S, *J ApplElectrochem*, 17 (1987) 828.
14 Da Silva L M, De Faria L A, Boodts J F C, *J ElectroanalChem*, 141 (2002) 532.
15 Tavares A C, Cartaxo M A M, Da Silva Pereira M & Costa F M, *J Solid State Electrochem*, 5 (2001) 57.
16 Nikilov I, Darkaoui R, Zhecheva E, Stoyanova R, Dimitrov N &Vitanov T, *J ElectroanalChem*, 429 (1997) 157.
17 Lee Yuh-Shu, Hu Chi-Chang & Wen Jen-Chen, *J ElectrochemSoc*, 143 (4) (1996) 1218.

18 Iwakura C, Nishioka M & Tamura H, *Nippon Kagaku Kaishi*, 7 (1982) 136.
19 Iwakura C, Honji A & Tamura H, *ElectrochimActa*, 26 (1981) 1319.
20 Rasiyah P &Tseung A C C, *J ElectrochemSoc*, 130 (1983) 365.
21 Orehotsky J, Huang H, Davidson C R & Srinivasan S, *J ElectroanalChem*, 95 (1979) 233.
22 Zhou J, Ma J, Sun C, Xie L, Zhao Z & Tian H, *J Am Ceram Soc*, 88 (2005) 3535.
23 Yang J M, Tsuo W J & Yen F S, *J Solid State Chem*, 145 (1999) 50.
24 Singh N K, Tiwari S K, Anitha K L & Singh R N, *J ChemSocFaraday Trans*, 92(13) (1996) 2397.
25 Li Guo-Hui, Dai Li-Zhem, Lu Da Shun & Peng Shao-Yi, *J Solid State Chem*, 89 (1990) 167.
26 Bo C, Li J B, Han Y S & Dai J H, *Materials Lett*, 58 (2004) 1415.
27 Bocca C, Barbucci A, Deluchi M &Ceriola G, *Int J Hydrogen Energy*, 24 (1999) 21.
28 Bocca C, Ceriola G, Magnone E &Barbucci A, *Int J Hydrogen Energy*, 24 (1999) 699.
29 Baydi M El, Poillerat G, Rehspringer J L, Gautier J L, Koenig J F &Chartier P, *J Solid State Chem*, 109 (1994) 281.
30 Martin J L, Vidales Se, Garcia O Martinez, Vila E, Rojas R N &Torralvo M J, *Mat Res Bull*, 28 (1993) 1135.
31 Serebrennikova I &Briss V I, *J Mater Science*, 36 (2001) 4331.
32 Baydi M El, Tiwari S K, Singh R N, Koenig J F &Poillerat G, *J Solid State Chem*, 116 (1995) 157.
33 Singh N K, Singh J P & Singh R N, *Int J Hydrogen Energy*, 27 (2002) 895.
34 Svegl F, Orel B, Svegl I Grabec&Kaucic V, *ElectrochimActa*, 45 (2000) 4359.
35 Singh R N, Singh N K & Singh J P, *ElectrochimActa*, 47 (2002) 3873.
36 Singh R N, Singh N K, Singh J P, Balaji G &Gajbhiye N S, *Int J Hydrogen Energy*, 31 (2006) 701.
37 Singh J P, Singh N K & Singh R N, *Int J Hydrogen Energy*, 24 (1999) 433.
38 Singh R N, Singh J P, Lal B & Singh A, *Int J Hydrogen energy*, 32 (2007) 11.
39 Singh N K & Singh R N, *Ind J Chem*, 38A (1999) 491.
40 Singh R N, Singh J P & Singh A, *Int J Hydrogen Energy*, 33 (2008) 4260.
41 Tiwari S K, Chartier P & Singh R N, *J ElectrochemSoc*, 142 (1995) 148.
42 Gillot B, Laarz M &KacimS, *J Mater Chem*, (7) 827 (1997).
43 Gillot B, Nivoix V, Kester E, Nusillard O, Villete C, TailhadesPh&Rousset A, *Mater ChemPhys*, 48 (1997) 111.
44 Okasha N, *Mater ChemPhys*, 84 (2004) 63.
45 Fradette N & Marsan B, *J ElectrochemSoc*, 145 (1998) 2320.
46 Iwakura C, Nishioka M & Tamura H, *Denki Kagaku*, 49 (1981) 355.
47 Orehotsky J, Huang H, Davidson C R & Srinivasan S, *J ElectroanalChem*, 95 (1979) 233.
48 Al-Hoshan M S, Singh J P, Al-Mayouf A M, Al-suhybani A A&Shaddad M N, *Int J ElectrochemSci*, 7 (2012) 4959.
49 Gileadi E, *Electrode Kinetics*, (VCH Publishers Inc., New York), 1993 p.151.